Iranian Society of Acoustics and Vibration
The 12th ISAV2022 International Conference on Acoustics and Vibration
14-15 Dec 2022 Tehran - Iran
Amirkabir University of Technology

Effects of Geometrical Factors on Sound Silencing Behavior of Mass Attached Membrane-Type Acoustic Metamaterials

Seyyedmohammad Aghamiri[a], Mohammad J. Mahjoob[b],
Reza Ghaffarivardavagh[c], Farzad A. Shirazi[d*]

[a] *Master's student, School of Mechanical Engineering, College of Engineering, University of Tehran, Tehran, Iran*

[b] *Professor, School of Mechanical Engineering, College of Engineering, University of Tehran, Tehran, Iran*

[c] *Research Scientist, MIT Media Lab, Massachusetts Institute of Technology, Cambridge, MA, USA*

[d] *Assistant Professor, School of Mechanical Engineering, College of Engineering, University of Tehran, Tehran, Iran*
** Corresponding author e-mail: fshirazi@ut.ac.ir*

Abstract

Membrane-type acoustic metamaterials have attracted significant attention in recent years due to their capacity to generate low-frequency band gaps. To date, numerous analytical and numerical approaches have been developed to study and evaluate the acoustic performance of this type of metamaterial toward improving their sound silencing behavior. This paper examines different geometrical factors of the mass-attached membrane, including the thickness and pretension of the membrane, the weight, and the radius of the attached mass by using the pointwise matching method and a coupled analytical vibroacoustic analysis to determine the transmission loss of the metamaterial. We investigate how these geometrical factors contribute to sound silencing. Additionally, the full-wave simulation of these mass-attached membranes is carried out to validate the results numerically. The paper herein provides insight into how the geometrical parameters of mass-attached membranes can be tuned to broaden the silencing bandwidth and lower the frequency of the transmission loss peak in order to control low-frequency noise.

Keywords: Membrane-type acoustic metamaterial, frequency bandwidth, low-frequency regime, transmission loss, anti-resonance frequency

1. Introduction

Noise and unwanted sound are significant contributors to environmental pollution. This pollution can seriously affect people's daily lives, and if they are exposed to it for extended periods of time, they can suffer both physical and psychological harm [1]. Today, low-frequency noise is a problem that conventional acoustic materials cannot mitigate. Researchers have recently developed a new category of materials called metamaterials that are synthetic and unnatural. Acoustic metamaterials are new kinds of artificial materials composed of microstructures whose dimensions are smaller than the wavelength of incident sound waves. First, electromagnetic metamaterials were developed, followed by acoustic metamaterials. The similarity between light and sound waves makes acoustic metamaterials a natural transition from electromagnetic metamaterials [2].

One of the main challenges in existing research, especially in areas such as energy harvesting, is extending the frequency bandwidth of systems. Some examples are provided below. Based on their nonlinear characteristics, improving the bandwidth and power output of energy harvesting systems is still being studied [3]. The sound wave energy harvesting systems have few practical applications [4] because of the system's instability in the presence of waves with variable frequencies and sound pressure levels outside its operational range. Researchers should consider extending the bandwidth and increasing the amount of harvested energy in future research. As mentioned in [5], through the fluid-structure interaction analysis in the software as well as experimental tests inspired by the basilar membrane, a characteristic of frequency selection for acoustic sensors was developed, but the very narrow frequency band poses a major challenge. Membrane-type acoustic metamaterials are of particular interest in noise control due to their very low weight and significant capability in suppressing sound in low-frequency regimes [6]. These metamaterials are no exception to the issue of narrow bandwidth, and research has been conducted in order to widen their bandwidth. Figure 1 illustrates examples of geometry change methods from previous research.

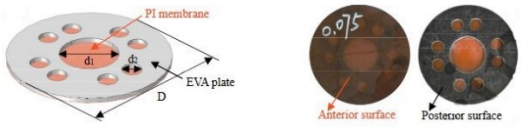

a) Placing a polymer sheet on the membrane surface [7]

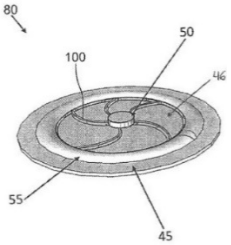

b) Adding concentric and curved objects on the circular membrane [8]

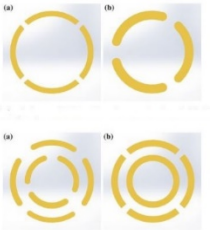

c) Different types of mass distribution over the circular membrane [9]

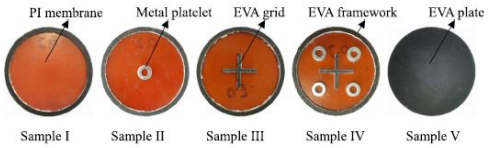

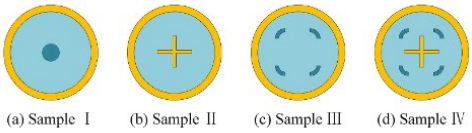

d) Using polymer masses (pure polyamide) with different shapes on the circular membrane [10] and [11]

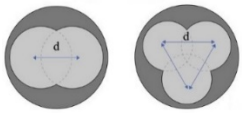

e) Two changes made in the geometry of the circular membrane [12]

Figure 1. Research has been conducted in order to broaden the operative frequency bandwidth of membrane-type acoustic metamaterials.

In articles [7], [10], and [11], the results of finite element simulations and experimental tests demonstrate that improving bandwidth has yielded favorable results. These articles all exhibit a single peak frequency on their transmission loss diagrams. Furthermore, no analytical modeling method has been used in these articles. Given these limitations, some studies on effective parameters cannot be conducted. The current research aims to use analytical tools to investigate the acoustic behavior of this type of metamaterial. This tool will be used to investigate widening the bandwidth and removing noise at low frequencies.

The metamaterial studied in this research consists of a membrane to which a rigid mass is attached. Here, the method presented in [13] is used as the basis for the analytical approach. An acoustic metamaterial of the membrane type is shown in Figure 2. Taking into consideration the forces between the rigid mass added to the membrane as well as its translational and rotational motion, a vibroacoustic analysis has been conducted in this article. Finally, to evaluate the system's acoustic performance, a sound transmission coefficient is calculated. The method presented in the mentioned research is the most comprehensive analytical method for solving the eigenvalue problem and vibroacoustic analysis of membranes with a rigid mass attached to them.

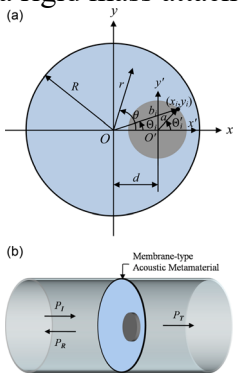

Figure 2. Membrane-type acoustic metamaterial. a) Front view of a membrane with an eccentric mass. b) Isometric view of a unit cell of metamaterial [13].

2. Method

The first step will be to present a theoretical model. A finite element model will then be introduced in order to verify the theoretical model. Accordingly, ANSYS Workbench is considered a tool for performing finite element analysis.

2.1 Theoretical Model

The membrane is stretched by applying a pretension over its outer boundary and is attached to the wall of the tube rigidly. In order to obtain natural frequencies and mode shapes of the membrane

and the attached mass, an eigenvalue problem has to be resolved. This paper employs the point matching method to capture the inertial effects of the mass attached to the membrane [13]. By using a specified number of point forces distributed along the inner boundary of the membrane, the equation governing motion of the membrane can be written as

$$\rho_s \frac{\partial^2 w(x,y,t)}{\partial t^2} - T\nabla^2 w(x,y,t) = \sum_{i=1}^{I} Q_i(t)\delta(x-x_i)\delta(y-y_i) \tag{1}$$

where, $w(x,y,t)$ is the out-of-plane displacement of the membrane in the z direction, and ∇^2 is the indicator of the Laplacian operator. On the right-hand side, I indicates the number of point forces or collocation points around the attached mass, and δ is the Dirac delta function. Eq. (1) will be solved in the steady-state field; hence, the time factor $e^{i\omega t}$ can be omitted, and the equation can be rewritten in polar coordinates as

$$\alpha^2 w(r,\theta) + \frac{\partial^2 w(r,\theta)}{\partial r^2} + \frac{1}{r}\frac{\partial w(r,\theta)}{\partial r} + \frac{1}{r^2}\frac{\partial^2 w(r,\theta)}{\partial \theta^2} = -\sum_{i=1}^{I} N_i \frac{b_i}{r}\delta(r-b_i)\delta(\theta-\Theta_i) \tag{2}$$

where $\alpha^2 = \rho_s\omega^2/T$, $N_i = Q_i/b_iT$, $b_i = \sqrt{a^2 + 2ad\cos(\Theta_i') + d^2}$, and $\Theta_i = \cos^{-1}[d + a\cos(\Theta_i')/b_i]$. According to [10], natural frequencies and mode shapes can be obtained by solving this equation.

In order to investigate the acoustic performance of the membrane with an attached mass, a coupled vibroacoustic problem must be solved. A plane sound wave strikes the membrane normally and causes it to have a transverse displacement denoted by w. The incident sound wave will be divided into two plane waves, reflected and transmitted. The left side of the membrane's pressure field is denoted by p_1, whereas the right side is designated by p_2. Now, the governing equation of the membrane excited by sound waves can be written as

$$-\omega^2\rho_s w - T\nabla^2 w = p_1|_{z=0} - p_2|_{z=0} + \sum_{i=1}^{I} Q_i\delta(x-x_i)\delta(y-y_i) \tag{3}$$

By considering continuous velocity condition, the distinction between average displacement and displacement deviation, rigid boundary condition along the inner side of the tube, and divergence theorem with Green's function, which is described in [13] in detail, the sound transmission coefficient can be derived as:

$$\tilde{T} = \frac{P_T}{P_I} = \frac{i\omega\rho_a c_a \langle w\rangle}{P_I} \tag{4}$$

where P_T is transmitted sound pressure, P_I is incident sound pressure, ρ_a and c_a are density and sound velocity in air, and $\langle w\rangle$ is the average value of the membrane's displacement. The sound intensity coefficient can be described as:

$$T_I = \left|\tilde{T}\right|^2 \tag{5}$$

Sound transmission loss is a widely used parameter in acoustics to assess the performance of noise control systems. This parameter may be expressed as follows based on the sound intensity coefficient:

$$STL = 10log_{10}\frac{1}{T_I}(dB) \tag{6}$$

2.2 Finite Element Model

ANSYS Workbench is used to perform finite element analysis in order to compare the results obtained by analytical modeling. In order to perform an acoustic analysis, static analysis should be performed first, and its output should then be used as an input to the acoustic analysis. For meshing the membrane, shell elements are used, as well as solid elements for modeling the connected solid mass. A membrane's outer boundary is fixed in the direction of the z-axis and around the z-axis, but it remains free in the direction of the radius. This is due to the fact that pretension is applied along the radius. A normal velocity excitation is used at the entrance of the pipe in order to produce and

spread plane waves in the tube. Its linear and back-and-forth movement acts like a piston at the beginning of the tube, causing a plane wave to travel along its length. Fluid-structure interaction boundary conditions are applied at the point of contact between membrane and air on both sides. This tube has a rigid wall, and the boundary condition of full absorption is used at its two ends so that no sound waves are reflected into the tube from either end. Figure 3 shows an exploded view of the membrane with central attached mass and the air. Table 1 presents information regarding the properties of the materials used, the amount of pretension, and the parameters relating to the attached rigid mass. These parameters will be considered as the base model.

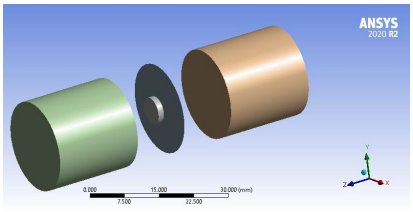

Figure 3. Exploded view of a membrane-type acoustic metamaterial unit cell in Ansys Workbench software. The cylinders around the membrane represent air as the medium for sound transmission.

Table 1. Membrane and the attached mass material properties and parameters [13].

Properties	Membrane	Mass
Mass density (kg/m^3)	980	7850
Young's modulus (Pa)	2×10^5	2×10^{11}
Poisson ratio	0.49	0.33
Thickness (mm)	0.28	-
Total weight (mg)	-	300
Radius (mm)	10	3
Pretension (N/m)	51.2	0

3. Results and Discussion

First and foremost, the frequency bandwidth within which the sound transmission loss is more significant than 20 dB will be considered a target parameter in this study to evaluate the performance of the membrane-type acoustic metamaterial. Thus, the acoustic intensity transmission coefficient will be less than one percent in such a bandwidth. Moreover, this value indicates a hundred-fold reduction in the energy and sound power produced by the source. The second parameter that will be considered to measure acoustic performance is the lower frequency at which the transmission loss peak occurs. The importance of noise control at low frequencies has led to the selection of this parameter as a target parameter. In the current study, no threshold has been established as low frequency, and only the reduction in the frequency of the transmission loss peak will be assessed.

3.1 Validation of the Theoretical Modelling

Figure 4 illustrates the results of acoustic analysis based on analytical equations and finite element simulations for the base model. There is a high degree of agreement between the two methods, which indicates that the analytical method is accurate and efficient. The figure shows that the transmission loss reaches its lowest value at two frequencies, 146 and 981 Hz corresponding to the system's resonance frequencies. A peak frequency of 269 Hz is also present between these two resonance frequencies. There is a 1.13% difference between the peak frequency reported in [13] and the value

obtained in this study, which is negligible. This peak frequency is also known as anti-resonance frequency.

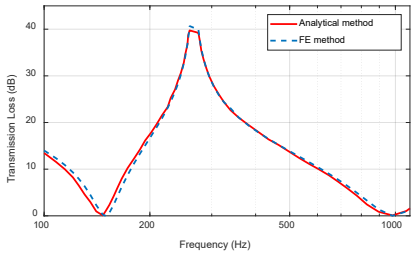

Figure 4. A comparison of analytical and finite element models of membrane-type acoustic metamaterials with central mass.

3.2 The Study of Geometrical Parameters of Membrane with Centric Attached Mass

In this section, we examine how the geometrical parameters of the membrane and the attached mass affect the bandwidth where the transmission loss exceeds 20 dB. It will also be investigated whether reducing the amount of anti-resonance frequency is possible. The geometrical parameters studied are the weight of the attached mass, the radius of the attached mass, the thickness of the membrane, and the pretension of the membrane. It is important to note that the pretension of the membrane is a microstructure effect; however, in this study, it is considered along with other geometrical effects.

Table 2 provides a comprehensive analysis of the geometric parameters. In this table, the first to third natural frequencies, anti-resonance frequencies, and the bandwidth with a transmission loss exceeding 20 dB have been calculated with several changes to geometric parameters. In Figure 5, we depict an example of the acoustic response (transmission loss) of the base model, whose parameters have been described in Table 1.

Table 2. Effects of different geometrical parameters on resonance and dip frequencies (Hz) of centric mass

Parameters	Values	1st resonance(Hz)	Dip frequency(Hz)	2nd resonance(Hz)	3rd resonance(Hz)	Over 20dB bandwidth(Hz)
Mass Weight(mg)	50	307	587	1021.6	1993	123.7
	100	236.2	444	994.1	1964	141.07
	150	198.8	371	983.2	1955.7	148.5
	200	175.1	326	977.6	1952	153.19
	250	158.1	293	974	1949.9	156.3
	300	145.2	269	971.6	1948.4	159
Mass Radius(mm)	1.5	117.4	170	780.5	1590.3	81.4
	2	126.1	196	838.1	1695.7	102.2
	2.5	136	230	901	1815	127.2
	3	145.2	269	971.6	1948.4	158.6
	3.5	154.6	314	1050.7	2101	198.31
	0.18	147	271	1206.3	2427.2	164.92

Membrane Thickness(mm)	0.2	146.4	270	1145.5	2303	163.73
	0.22	146.2	270	1093.1	2196.6	162.44
	0.24	145.8	269	1047.5	2103.5	161.24
	0.26	145.5	269	1007	2021	159.82
	0.28	145.2	269	971.6	1948.4	158.6
Membrane Pre-tension (N/m)	50	143.5	266	960.1	1925.4	155.27
	55	150.5	279	1007	2019.4	170.49
	60	157.2	291	1051.8	2109.2	185.61
	65	163.6	303	1094.7	2195.3	200.61
	70	169.8	314	1136	2278.1	215.54

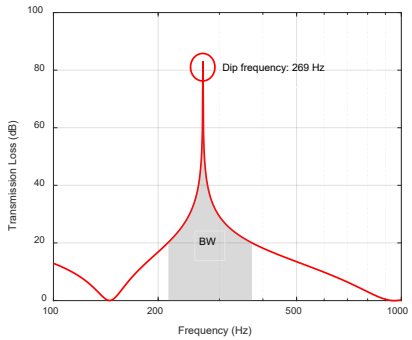

Figure 5. Transmission loss diagram of the base model. A peak transmission loss frequency and the bandwidth within which the loss exceeds 20 dB can be seen in this figure.

The table clearly illustrates that with an increase in the weight of the attached mass, the anti-resonance frequency has decreased by approximately 54%, while the desired bandwidth has also increased by approximately 29%. The changes are very beneficial since the peak frequency is reduced, and the frequency bandwidth is increased.

As the radius of the attached mass increases, while the weight remains constant, the desired bandwidth has increased significantly by 144%. However, the amount of anti-resonance frequency has increased as well to 85%. Even though it is not desirable to increase the anti-resonance frequency, it is important that it remains in a low-frequency regime.

The membrane thickness has been changed from 0.18 mm to 0.28 mm, which is the thickness value in the base model. Changing the membrane thickness does not appear to significantly affect bandwidth and anti-resonance frequency. The membrane is not capable of withstanding bending. Consequently, the thickness of the membrane, which can have an effect on bending stiffness, has no impact on the parameters studied. As a result, if frequency changes are required for the second and third resonances of the system during the design process, but the bandwidth or the anti-resonance frequency remains unchanged, increasing the thickness of the membrane may provide a solution.

In Table 2, the pretension in the membrane is the last geometrical parameter examined. The table indicates that the bandwidth has grown by 39%, and the anti-resonance frequency has increased by 18%. Although it is evident that an increase in anti-resonance frequency is not desirable, it is important to note that its value remains at low frequencies, which is generally desirable. Furthermore, the increasing rate of the bandwidth is greater than that of the anti-resonance frequency.

4. Conclusion

In order to quantitatively analyze the performance of the membrane-type acoustic metamaterial, two target parameters were defined. The first parameter was the bandwidth at which the transmission loss exceeds 20 dB, and the second parameter was the anti-resonance frequency value. Except for the weight of the attached mass, all parameters have experienced similar changes. This means that the anti-resonance frequency has increased with the increase in bandwidth. By changing the weight of the attached mass, target parameters change against each other. With increasing weight, the bandwidth increases while the anti-resonance frequency decreases. Additionally, the percentage changes indicate that the anti-resonance frequency decreases more rapidly than the bandwidth growth rate. In comparison with other geometric parameters, this behavior is the most desirable. As the radius of the attached mass increases, both target parameters increase; however, bandwidth increases at a much faster rate than anti-resonant frequency increases. Based on the changes in the target parameters obtained by increasing the membrane thickness, it can be concluded that this geometric parameter has an insignificant effect on the target parameters. It appears that the cause of this is the minor effect of bending stiffness on membranes. An increase in membrane pretension results in an increase in anti-resonance frequency and bandwidth. Increasing the bandwidth, in this case, occurs more rapidly than increasing the anti-resonance frequency.

REFERENCES

1. Münzel, Thomas, et al. "The adverse effects of environmental noise exposure on oxidative stress and cardiovascular risk." Antioxidants & redox signalling **28.9**, 873-908 (2018).
2. Cummer, Steven A., Johan Christensen, and Andrea Alù. "Controlling sound with acoustic metamaterials." Nature Reviews Materials **1.3** 1-13 (2016).
3. Safaei, Mohsen, Henry A. Sodano, and Steven R. Anton. "A review of energy harvesting using piezoelectric materials: state-of-the-art a decade later (2008–2018)." Smart Materials and Structures **28.11** 113001 (2019).
4. Choi, Jaehoon, Inki Jung, and Chong-Yun Kang. "A brief review of sound energy harvesting." Nano energy **56** 169-183 (2019).
5. Kim, Yooil, Ji-Sik Kim, and Gi-Woo Kim. "A novel frequency selectivity approach based on travelling wave propagation in mechano-luminescence basilar membrane for artificial cochlea." Scientific reports **8.1** 1-8 (2018).
6. Lu, Zhenbo, et al. "Membrane-type acoustic metamaterial with eccentric masses for broadband sound isolation." Applied Acoustics **157** 107003 (2020).
7. Zhou, Guojian, et al. "An approach to broaden the low-frequency bandwidth of sound insulation by regulating dynamic effective parameters of acoustic metamaterials." Journal of Physics D: Applied Physics **52.21** 215102 (2019).
8. US patent No. 8,752,667 (McKnight. G. P., Chang, C. M. 2014)
9. Xu, Ruochen, and Zhenbo Lu. "Eccentric Mass Designs of Membrane-Type Acoustic Metamaterials to Improve Acoustic Performance." IRC-SET 2018. Springer, Singapore, 275-288 (2019).
10. Zhou, Guojian, et al. "Broadband low-frequency membrane-type acoustic metamaterials with multi-state anti-resonances." Applied Acoustics **159** 107078 (2020).
11. Huang, Yonghu, et al. "Sound insulation properties of membrane-type acoustic metamaterials with petal-like split rings." Journal of Physics D: Applied Physics **55.4** 045104 (2021).
12. Watanabe, Keita, Mikiya Fujita, and Kenji Tsuruta. "Design of non-circular membranes meta-surfaces for broadband sound absorption." Japanese Journal of Applied Physics **59.SK** SKKA06 (2020).
13. Chen, Yangyang, et al. "Analytical coupled vibroacoustic modelling of membrane-type acoustic metamaterials: Membrane model." The Journal of the Acoustical Society of America **136.3** 969-979 (2014).